

EFFECT OF T56 PRESWIRL COOLING MODELLING ON DISC ASSEMBLY TEMPERATURE PREDICTION

Thomas Roos and Eu'odia Kruger

CSIR, P O Box 395

Pretoria, 0001, South Africa

Tel: +27 12 841-2329

Fax: +27 12 349-1156

throos@csir.co.za

ABSTRACT

The T56 Series III 1st stage rotor blade is cooled using moderately preswirled air from 36 preswirl injection nozzles. The amount of swirl achieved by discrete preswirl coolant jets is generally unknown, due to mixing losses. A "frozen-rotor" CFD analysis was therefore performed on a sector of the NGV support plate/1st stage rotor disc cavity of the T56 turboprop engine, including a preswirl injection hole and a section of the upstream plenum. It was found for this geometry that the mean tangential velocity of the coolant in the preswirl region of the rotor-stator cavity was about half the maximum tangential velocity in the preswirl jets ($C_{\theta\text{mean}}/C_{\theta\text{maxjet}} = 0.5$). This value was used in ICP, a one-dimensional coolant flow network program, to model coolant flow in the disc cavities. ICP was then iterated with the disc assembly conduction code DCOOL to obtain the temperature distribution in the disc assembly. The result was compared with the resultant temperature distribution for a $C_{\theta\text{mean}}/C_{\theta\text{maxjet}}$ value of unity. The temperature distribution in most of the 1st disc remained largely insensitive to the value of $C_{\theta\text{mean}}/C_{\theta\text{maxjet}}$, showing the spacer to play a greater role in heat conduction to the disc than the blade shanks.

NOMENCLATURE

3-D	3-Dimensional
CAD	Computer Aided Drawing
CFD	Computational Fluid Dynamics
DCOOL	3-D finite difference conduction solver for disc assemblies
FEM	Finite Element Method
ICP	Compressible one-dimensional network-type coolant flow solver
NGV	Nozzle Guide Vane
OEM	Original Equipment Manufacturer
SAAF	South African Air Force
C_{θ}	Preswirl air tangential velocity
$C_{\theta\text{maxjet}}$	Maximum C_{θ} in preswirl jet
$C_{\theta\text{mean}}$	Mean C_{θ} in cavity

INTRODUCTION

Rolls Royce, the OEM of the T56/501D turbo-prop engine family, reduced the authorised service life of various components of the engine (rotor disc 1 in Series II and the 1-2 spacer in Series III). This led to a requirement by the South African Air Force (SAAF) that the CSIR perform life assessment studies on these components. A necessary input to life assessment studies is a disc cavity heat transfer analysis, including disc coolant

flowfield analysis and disc cavity component temperature distribution calculation. These were then to be used in a detailed FEM model for life assessment prediction.

Heat transfer prediction challenges

The T56 disc assembly flowfield involves the following:

- The NGV support plate/1st disc rotor-stator cavity, involving preswirl injection jets (requiring detailed modelling)
- 3 upstream disc/downstream spacer rotor-rotor cavities, involving choked inlet flow jets (requiring detailed modelling) through metering holes in the rotor disc and outlet flow through scallops in the spacer rim
- 2 upstream spacer/downstream disc rotor-rotor cavities, involving choked inlet flow jets (requiring detailed modelling) through metering holes in the rotor disc and outlet flow through the rotor blade shanks at the disc rim
- The unventilated cavity between the 3-4 spacer and the 4th disc
- 3 rotor-rotor cavities inboard of the rotor-rotor curvic couplings
- hot gas flowpath heat transfer to the platforms of the blades on all 4 discs
- hot gas flowpath leakage flow through the stator blade ring/spacer labyrinth seals and the rotor stator cavities up- and downstream of the labyrinth seals.

Only a simplified analysis using empirical heat transfer models of various types of flows together with and a 3D conduction model could be used to model the entire assembly (4 discs, 3 spacers, multiple blade root shank flows, metering holes and cavity exhaust scallops) rapidly, varying the boundary conditions for each run. Modelling portions of the assembly for life assessment does not make sense as thermal conduction takes place at the contact boundaries between discs and between discs and spacers, the entire assembly must be modelled. On the other hand, where empirical heat transfer models of certain types of flow are not currently available such as the inclined metering hole impingement flow and the resultant cavity flowfield, or the preswirl cooling flowfield, only CFD or detailed experimental investigations can provide the required answers.

An equivalent CFD model of the entire assembly would be clearly intractable if any

accuracy regarding heat transfer was to be expected, as the mesh would have to resolve thermal boundary layers, three-dimensional (non-axisymmetric) effects such as jets as well as solve conjugate heat transfer. An 800 000 cell grid would be the minimum grid size required to solve one of the 6 disc-spacer cavities, given the metering-hole flows. Then, in order to perform a life assessment, solutions would have to be obtained for many different points on the operating cycle to capture the effect of transients.

Approach followed

Because of the above, two numerical heat transfer analyses were then performed, one a simplified analysis of the whole assembly, the other a detailed CFD analysis of a subassembly. This twin-path approach was followed because no one tool available could perform the complete task.

In the first, a simplified numerical analysis, a one-dimensional coolant network solver, ICP, was used to model the coolant flow in the disc cavity regions of the T56 in 1999. A conduction model of the T56 disc assembly was built the following financial year using the 3-D disc assembly conduction code DCOOL. The ICP coolant flow and DCOOL conduction models have been continuously upgraded since then. ICP and DCOOL are described in Snedden *et al* (2005).

For the second, detailed type of analysis, Snedden (2003) describes the CFD analysis performed, where only a model of the cavity between the 1st disc and the 1-2 spacer was built and run. This CFD simulation concentrated on:

- The impingement flow from the metering hole, its effect on cooling the rotor disc in the hole and its effect on driving the flow in the cavity.
- The coolant flow exiting the cavity through the scallops at the outer radius of the 1-2 spacer and its effect on cooling both the rotor disc and the spacer as it passes through the constriction caused by the scallops.
- The radial and tangential thermal conduction through the disc and spacer.
- The heat transfer “footprint” on the disc and spacer.

The idea behind the twin-path approach was to modify the ICP-predicted heat transfer distribution to match the CFD results, and thereby create a quasi-empirical modification to be applied to the ICP-correlation for the T56 flows. This, when applied to a transient DCOOL disc assembly conduction model, would supply the results necessary for life calculation.

Preliminary results and research problem

A steady-state calculation of the disc assembly temperature distribution at the take-off condition was then performed using ICP and DCOOL. This analysis resulted in predictions of unrealistically low blade root and disc temperature distributions in the 1st stage disc relative to the other discs. Now the T56 Series III 1st stage rotor blade is cooled using moderately preswirled air from 36 preswirl injection nozzles, set at 40° to axial direction in the

axial-tangential plane. It was determined that the unrealistically low temperature predictions was due to the assumption in ICP that the swirl velocity in the rotor/stator cavity is equal to the swirl velocity in the pre-swirl jets at exit from the preswirl injection holes:

$$C_{\theta\text{mean}} = C_{\theta\text{maxjet}}$$

El-Oun and Owen (1989) showed that a radial outflow of coolant in a rotor/stator cavity from the disc centre, warmed by the disc, superimposed on the preswirl main coolant flow near the disc rim can cause the efficiency of a preswirl cooling system to deteriorate, firstly by slowing the tangential velocity of the preswirl flow and secondly by the mixture being heated by the addition of the warmed coolant. This mechanism was therefore subsequently added to ICP but the results obtained were still unrealistic.

Geis *et al* (2004) however showed that for a low number of preswirl injection nozzles (12 as opposed to 60 of El-Oun and Owen, 1989), quasi-axisymmetric flow cannot be assumed, and mixing losses reduce the cavity flow tangential velocity achievable. A decreased tangential coolant velocity increases the relative total temperature of the coolant entering the coolant admission holes in the disc.

In accordance with the modelling strategy described earlier, a CFD analysis of the 1st stage stator-rotor disc cavity was therefore required to determine the ratio of cavity coolant tangential velocity to the pre-swirl jet tangential velocity $C_{\theta\text{mean}}/C_{\theta\text{maxjet}}$, as input to the next ICP analysis. This paper describes that activity.

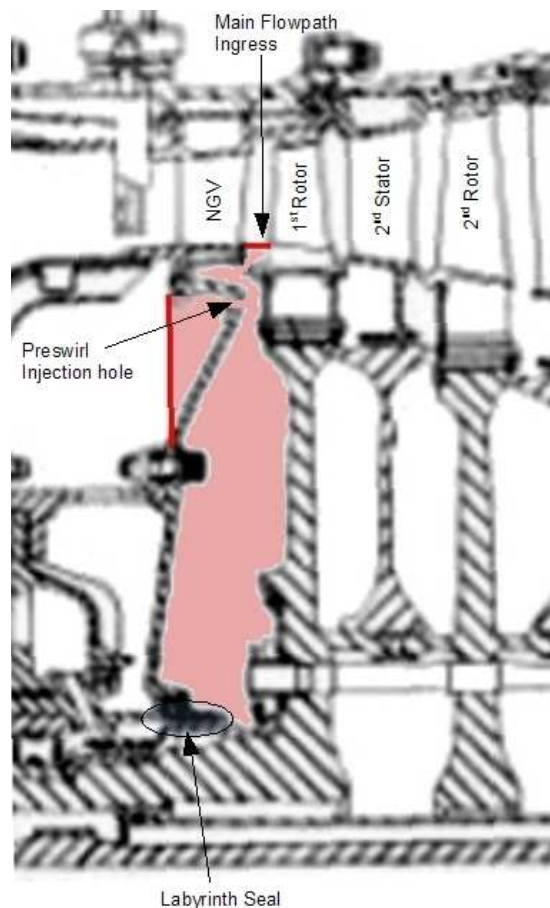


Figure 1: Meshed region of T56 disc assembly
PRESWIRL COOLING CFD ANALYSIS

Geometry

To perform a CFD analysis on a full 360° sector would prove computationally prohibitive. A sector was therefore sought that would contain an integer number of the relevant geometric features. This sector, with cyclic boundary conditions, would provide a representative solution. The numbers of dominant integer non-axisymmetric features are given in Table 1, as well as two possible sector choices.

Table 1: Integer number of features in geometry concerned

	Full 360°	1/36 sector	1/34 sector	Modelled sector
Rotor blade holes	102	102/36 = 2.833	102/34 = 3	3
Pre-swirl holes	36	36/36 = 1	36/34 = 1.059	1 (new diameter)
Cover-plate nuts	24	24/36 = 0.667	24/34 = 0.706	1 (new diameter)

In order to obtain the correct flowfield, the CFD analysis required for this project would have to include the full rotor-stator cavity bounded by the NGV support plate and the 1st stage rotor disc, including the labyrinth leakage flowpath boundary conditions, the full stationary and rotating walls and the hot gas flowpath.

It is very important to obtain realistic flow in the preswirl injection hole itself, since it drives the entire preswirl cooling process. As the injection hole is aligned at an angle of 40° to axial direction, the flow will separate where the hole wall makes an acute angle with the front face of the NGV support plate, causing a non-axisymmetric vena contracta. The inclusion of the section of plenum upstream of the hole allows this vena contracta to develop in the model, as the boundary conditions are moved away from the hole entrance. Figure 1 shows the regions modelled in colour.

As non-axisymmetric geometric details exist on both the stationary and rotating walls, a choice had to be made as to the use of a transient sliding mesh or a steady state “frozen rotor” approximation. The latter was chosen as the computational requirements are not so demanding and the results are still applicable.

As the temperature of the coolant in the rotating cooling hole in the rotor blade root was the ultimate aim, it was decided that exact modelling of the rotor blade cooling holes was required for accuracy. This gave the 1/34th sector as the preferred geometry, with the area of the upstream injection hole increased by 5.9% and the diameter of the NGV support plate nuts reduced (by keeping the blockage area ratio constant) to achieve equivalence with the full 360° case.

Boundary conditions

Boundary conditions were calculated from known OEM data. Boundary types were not always obvious, however. When a pressure boundary was initially applied at the three rotor blade coolant

admission holes, reverse flow back into the rotor-stator disc cavity occurred at one of the holes. A “frozen rotor” analysis is essentially steady-state, while the reality is transient. A fixed massflow boundary was then applied at the holes instead; giving a better representation of the flow since the passing frequency of the blade admission holes past the preswirl injection jet is more likely to give rise to a fluctuating pressure in the coolant admission holes than a fluctuating flow direction. Over time an equal amount of coolant is expected through each of the coolant holes, and this was enforced by boundary condition.

The pressure and temperature at the upstream plenum boundary was known as well as the massflow through the preswirl injection hole. The velocity at this inlet boundary was adjusted until the static pressure calculated for this region equalled that in the combustion chamber. The sides of the upstream plenum boundary were not chosen to be cyclic boundaries, but slip walls, to prevent spurious tangential velocities that take excessively many iterations to dissipate. The CFD geometry does not follow the exact T56 geometry at the top of the upstream plenum where the 1st stage stator tab slots into the NGV support plate, but is instead simplified from an inner lip at the outer wall to a simple cylindrical outer wall (see from Figure 1), as the extra detail was not considered justifiable as the velocities are very low there.

A fixed massflow boundary velocity was imposed at the labyrinth seal near the disc bore. At the hot gas flowpath interface with the stator-rotor cavity flowfield, the flow direction is determined by the upstream stator blade row. Velocity components were imposed at this pressure boundary to simulate the flow exiting the stator blade at the hub. The velocity values were estimated and assumed to be at 60° to the axial direction. This provides the tangential velocity component at the outer radius flowfield boundary.

RESULTS

Preswirl injection hole

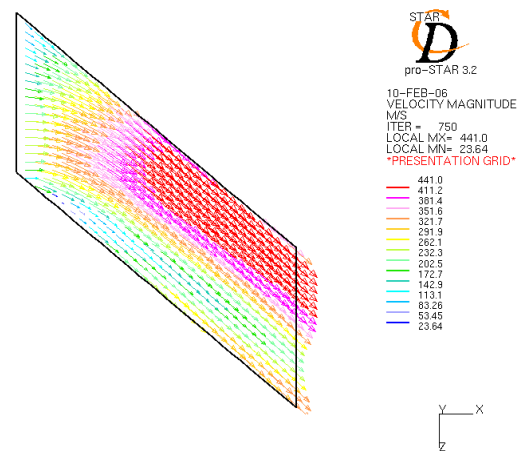


Figure 2: Vector section at central plane of preswirl injection hole.

Figure 2 shows a slice in the axial-tangential plane through the centre of the preswirl

hole. The separation from the wall is visible at the inlet to the hole. Figure 3 shows the velocity magnitude and temperature distributions at the outlet from the injection hole. The low-velocity core resulting from the separation at the hole inlet can be seen in both Figure 2 and Figure 3.

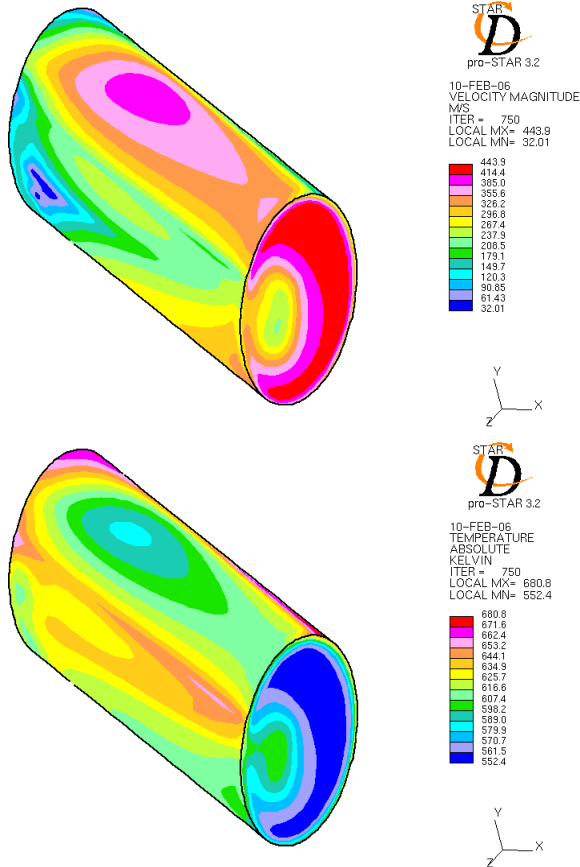


Figure 3: Velocity magnitude and temperature distribution at outlet from injection hole

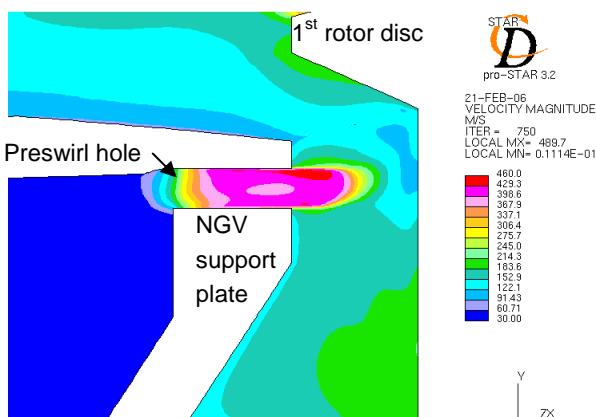


Figure 4: Velocity magnitude at slice through injection hole.

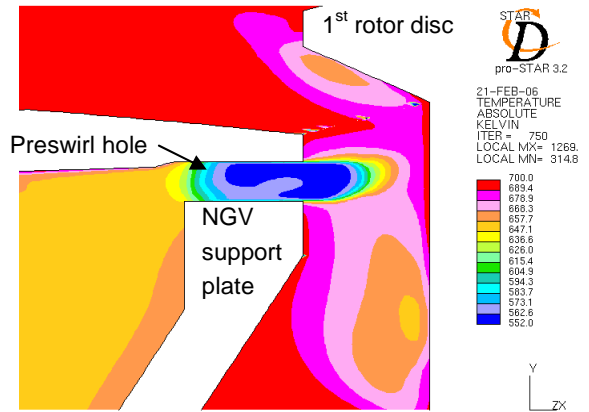


Figure 5: Temperature at slice through preswirl injection hole.

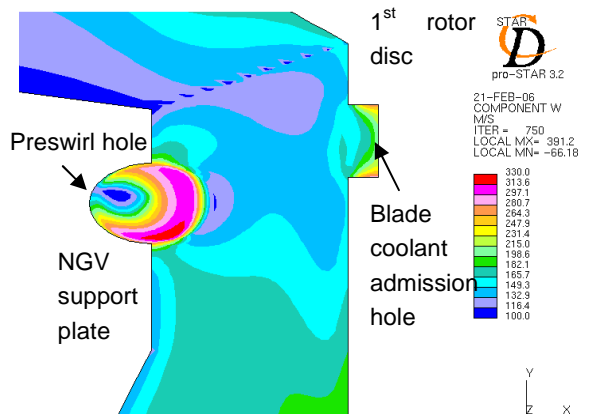


Figure 6: Tangential velocity at slice through injection and blade coolant admission hole.

Impingement region

Despite the strength of the injection jet (about 400m/s: see Figure 2), the essentially tangential velocity of the coolant in the cavity between the NGV support plate and the 1st stage rotor is much slower, at about 150m/s (see figures 4 and 6).

Correspondingly, the coolant temperature in the cavity between the NGV support plate and the 1st stage rotor (about 670K) is not anywhere near as low as in the jet (about 560K) but closer to the upstream plenum temperature of 650K (see figure 5).

Figure 6 shows the *tangential* velocity distribution at a different slice, cutting through one of the blade root coolant admission holes. Here the coolant tangential velocity in the cavity between the NGV support plate and the 1st stage rotor is seen to lie between 130m/s and 150m/s, about half the tangential velocity in the high-momentum part of the jet.

This is shown more clearly in Figure 7, a slice taken in the axial-tangential plane. Despite the tangential velocity in the high-momentum part of the jet exceeding 300m/s, it is only able to entrain the coolant in the cavity to a tangential velocity between 140m/s and 160m/s. The mean coolant temperature in the cavity at this radius appears to lie between 667K and 687K, all hotter than the plenum coolant temperature.

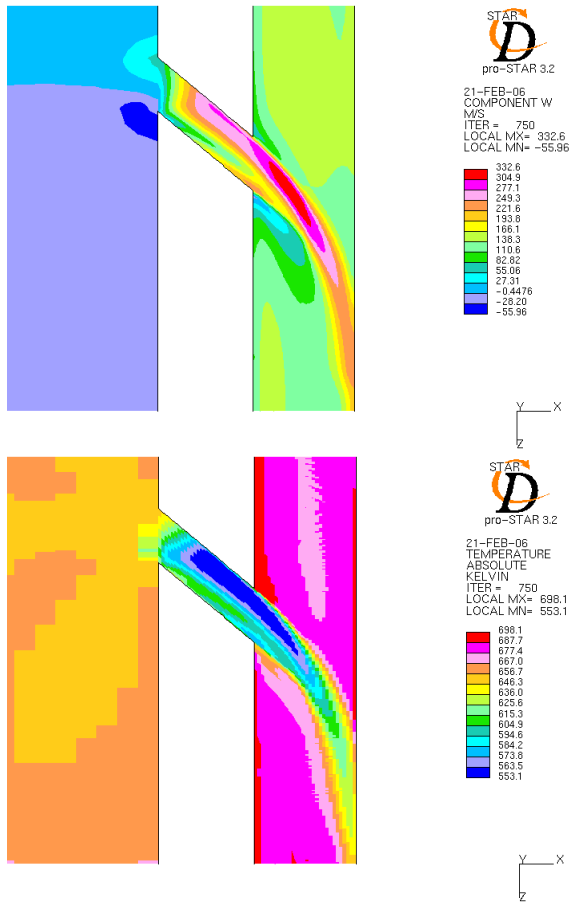


Figure 7: Tangential velocity and temperature in slice taken in the axial-tangential plane through preswirl hole

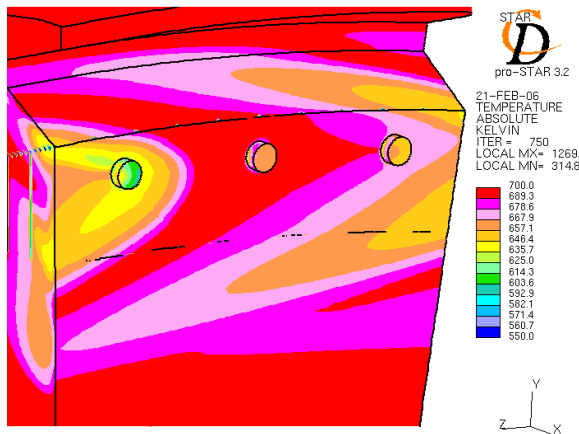


Figure 8: Coolant temperature footprint on 1st stage rotor disc

Better understanding can possibly be obtained from looking at Figure 8, which shows the impingement of the coolant jet on the 1st stage rotor disc, frozen at an instant. The coolant temperature at the centre of the impinging jet (which strikes the leftmost hole in figure 8) lies between 625K and 650K, lower than the plenum temperature. This shows at least some temperature drop due to preswirl. Outside the jet the coolant is hotter, but the temperature of the coolant entering the holes is

at or less than 650K on average.

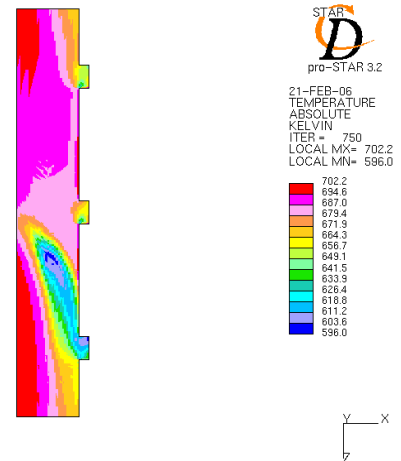


Figure 9: Coolant temperature distribution at axial-tangential slice through coolant holes

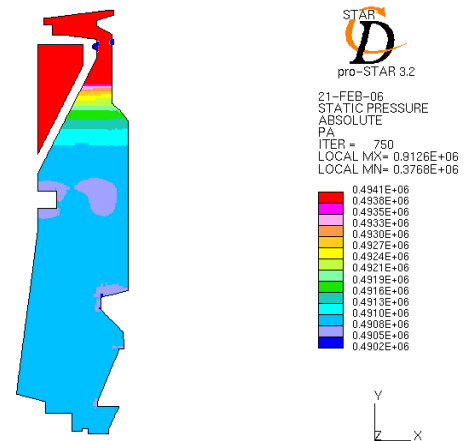


Figure 10: Pressure gradient in cavity

Figure 9 shows the coolant temperature distribution at an axial-tangential slice through the blade coolant admission holes. The footprint of the jet can be seen, and the temperature of the coolant entering the coolant holes is at or less than 650K on average. From the above it may be determined that as a fair rule of thumb, the mean coolant tangential velocity in the T56 NGV support plate-1st stage rotor disc cavity is about half that of the coolant jet maximum tangential velocity, or

$$C_{\theta \text{mean}} = 0.5 C_{\theta \text{maxjet}}$$

This relationship was then implemented in the ICP model to obtain a DCOOL temperature solution for the disc assembly. As a matter of interest, the static pressure gradient in the NGV support plate-1st stage rotor disc cavity is shown in Figure 10. It can be seen that a noticeable gradient is only discernable in the transition region between the cavity proper and the impingement jet region.

ICP/DCOOL analysis

The ICP model was modified such that the tangential velocity of the coolant in the preswirl region of the cavity was half that of the tangential velocity of the jet. ICP was then iterated with the

disc assembly conduction code DCOOL to obtain the temperature distribution in the disc assembly.

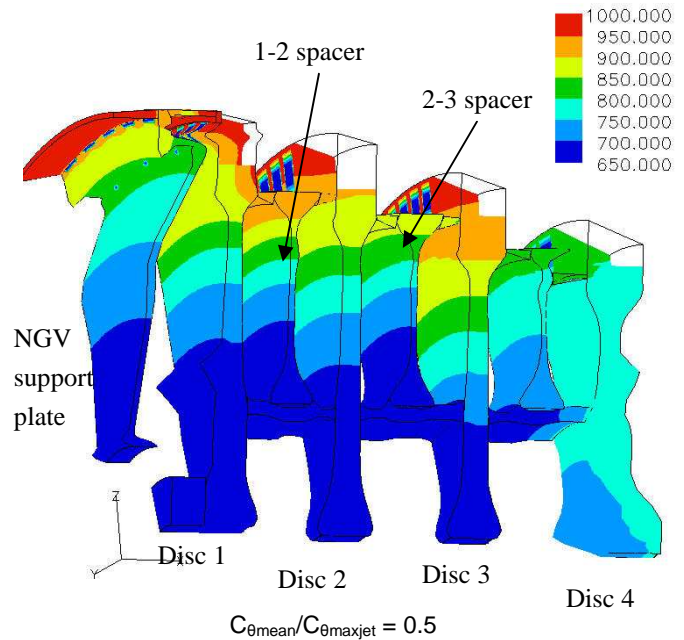
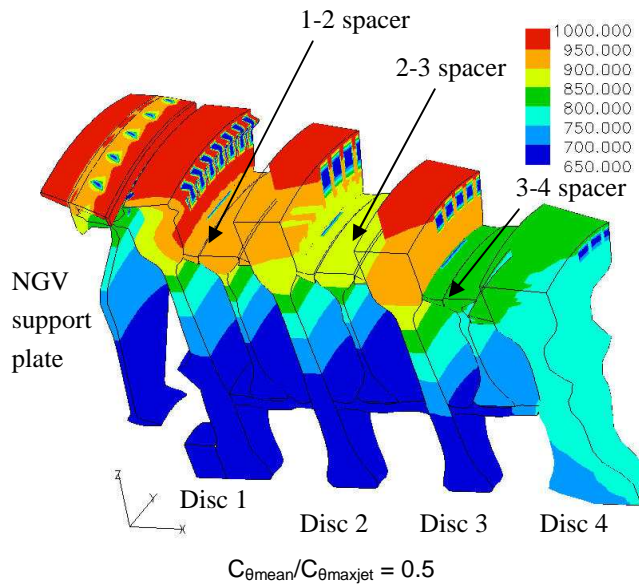
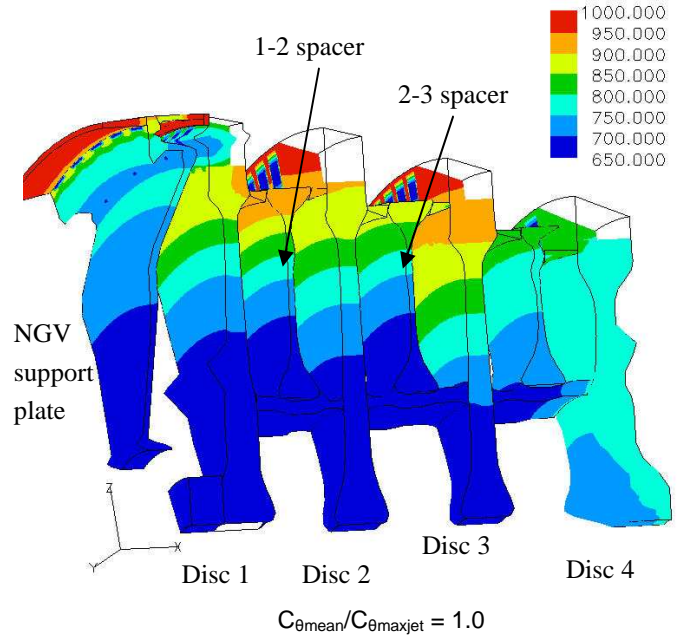
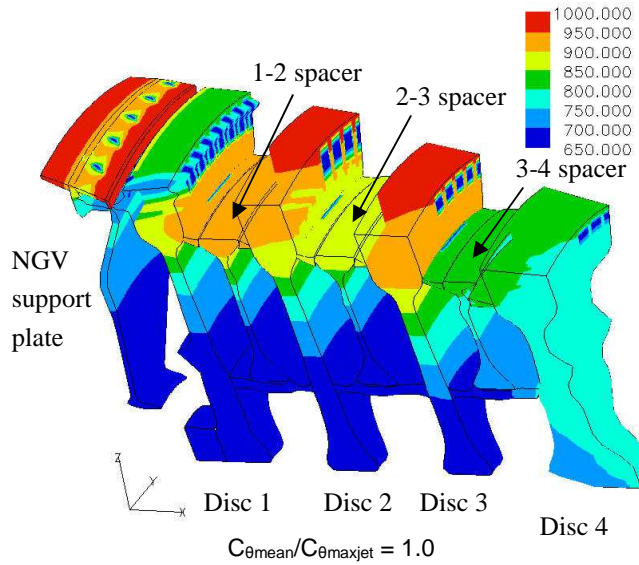


Figure 11: Comparison of disc assembly temperature distribution predictions in Kelvin for $C_{\theta\text{mean}}/C_{\theta\text{maxjet}}$ values of 1.0 and 0.5, viewed from above

Figure 12: Comparison of disc assembly temperature distribution predictions in Kelvin for $C_{\theta\text{mean}}/C_{\theta\text{maxjet}}$ values of 1.0 and 0.5, viewed from below

Figures 11 and 12 show comparisons of the temperature distribution predictions of the disc assembly sector for $C_{\theta\text{mean}}/C_{\theta\text{maxjet}}$ values of 1.0 and 0.5 with views from above and from below respectively. No blade aerofoils are shown, only the blade platforms, and several blade shanks are not shown in each blade row to display the disc rims. The blue rectangles in the rim of the disc are the spaces between the blade shanks containing coolant air (the blade root coverplates are not displayed). Similarly, the blue lines between the spacers and their upstream discs indicate the scalloped holes through which the cavity coolant air escapes.

The reduction in $C_{\theta\text{mean}}/C_{\theta\text{maxjet}}$ value from 1.0 to 0.5 led to an increase in the coolant temperature relative to the 1st stage rotor disc. The effect of the rise in coolant temperature is most visible in the 1st stage rotor disc temperature distribution at radii larger than the rim of the 1-2 spacer (the blade firtrees, shanks and platforms), leading to a platform temperature rise of the 1st stage rotor blades of some 150K. The 1st stage rotor blade platform temperature is now comparable to the NGV platform temperature. The NGV support plate temperature between the preswirl holes and the NGV platforms has increased some 100K. At radii less than the rim of the 1-2 spacer, however, the temperature distribution of the 1st stage rotor disc is practically unchanged.

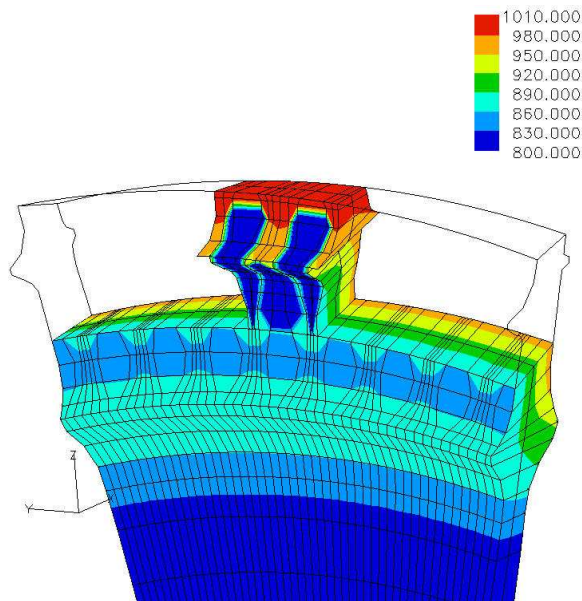


Figure 13: Shank and platform temperature distribution in Kelvin for two 1st stage rotor blades and 1st stage rotor disc for $C_{\theta\text{mean}}/C_{\theta\text{maxjet}} = 0.5$

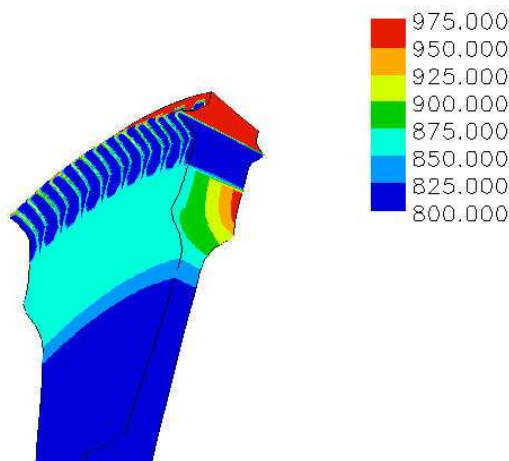


Figure 14: Detail of temperature distribution in fir-tree region of 1st stage rotor disc

This appears to indicate that the thermal input to the disc rim due to conduction through the blade shanks for this disc is not as significant a contributor to the disc temperature distribution as conduction from the adjacent spacer.

This is supported by examining the temperature predictions for a $C_{\theta\text{mean}}/C_{\theta\text{maxjet}}$ value of unity. The maximum temperature of the 1st stage rotor is adjacent the spacer. Figure 13 shows the temperature distribution in the shanks of the 1st stage rotor blades without the blade root coverplates, with the grid overlaid to assist the reader in interpreting the figure. A definite axial temperature gradient is visible in the lower blade shanks, similar to the disc fir-tree region. Figure 14 shows the axial temperature gradient in the fir-tree region using more close-spaced contours.

CONCLUSIONS

A "frozen-rotor" CFD analysis was performed on a sector of the NGV support plate /1st stage rotor disc cavity of the T56 turboprop engine,

including a preswirl injection hole and a section of the upstream plenum. It was found that the mean tangential velocity of the coolant in the preswirl region of the rotor-stator cavity was about half the maximum tangential velocity in the preswirl jets:

$$C_{\theta\text{mean}}/C_{\theta\text{maxjet}} = 0.5$$

This value was used in ICP. ICP was then iterated with the disc assembly conduction code DCOOL to obtain the temperature distribution in the disc assembly. The result was compared with the prediction of temperature distribution from a previous solution using a $C_{\theta\text{mean}}/C_{\theta\text{maxjet}}$ value of unity. Strangely enough, the temperature distribution in most of the 1st disc remained largely insensitive to the value of $C_{\theta\text{mean}}/C_{\theta\text{maxjet}}$. This appears to indicate that the thermal input to the disc rim due to conduction through the blade shanks for this disc is not as significant a contributor to the disc temperature distribution as conduction from the adjacent spacer.

Future work will involve validating ICP/DCOOL predictive capability with thermal paint results obtained in a previous project.

REFERENCES

El-Oun Z B and Owen J M (1989), "Preswirl Blade-Cooling Effectiveness in an Adiabatic Rotor-Stator System", Trans ASME Journal of Turbomachinery, Vol III, October 1989, pp 522-529

Geis T, Dittmann M and Dullenkopf K (2003), "Cooling Air Temperature Reduction in a Direct Transfer Preswirl System", ASME paper GT 2003-38231

Snedden G C (2003), "A CFD Analysis of the Impingement Cooling Effect of the Coolant Jet Caused by the T56 1st Stage Disc Metering Hole", ISABE-2003-1065

Snedden G C, Roos T H and Naidoo K (2003), "Detailed Disc Assembly Temperature Prediction: Comparison of CFD with Simplified Engineering Methods", ISABE-2005-1130

